ORIGINAL ARTICLE

Experimental synthesis of size-controlled TiO$_2$ nanofillers and their possible use as composites in restorative dentistry

Dipika V. Raorane [a,*], Ramesh S. Chaughule [a], Suhas R. Pednekar [b], Anushree Lokur [c]

[a] Department of Chemistry, Ramnarain Ruia Autonomous College, Matunga, Mumbai 400019, India
[b] University of Mumbai, Mahatma Gandhi Road, Fort, Mumbai, Maharashtra 400032, India
[c] Department of Microbiology, Ramnarain Ruia Autonomous College, Matunga, Mumbai 400019, India

Abstract The aim of this work was to obtain an efficient protocol with a green, fast and facile way to synthesize TiO$_2$ NPs and its application as fillers for enhancement of desired dental properties of light curing dental composites.

A comparative study comprised the fabrication of light curing restorative composite materials with incorporating different fillers with varying wt%, varying resin material composition, to determine optimal dental restoration by focusing on the physical properties of dental materials. It was observed that the as-prepared green synthesized TiO$_2$ nanohybrid particles contributed to the improvement in physical properties, thus promoting the green and rapid synthesis of nanohybrid fillers. In addition, mechanical values for experimental cured resin materials with bare and surface modified fillers were obtained. The experimental light curing nanocomposites with 5 wt% (wt%) nanohybrid surface modified filler particles with BisGMA (60 wt%), TEGDMA (20 wt%) and UDMA (20 wt%) resin composition provided increased physical strength and durability with higher compressive stress 195.56 MPa and flexural stress 83.30 MPa. Furthermore, the dental property, such as polymerization shrinkage (PS) obtained from volumetric method was decreased up to 3.4% by the addition of nano-hybrid fillers. In addition to this, the biocompatible and antimicrobial nature of TiO$_2$ and its aesthetics properties such as tooth-like color makes TiO$_2$ favorable to use as fillers.

* Corresponding author.
  E-mail address: raorane.dipika@gmail.com (D.V. Raorane).

This study presents a green and facile method for the synthesis of TiO$_2$ nanohybrid particles that can be successfully used as fillers in an experimental light curing resin matrix for enhancing its dental properties. This describes the potential of the green synthesized TiO$_2$ nanohybrid particles to use as fillers in restorative dentistry.

1. Introduction

Tooth decay or dental caries have historically been considered as a common oral problem and is still a public health concern (Prasai Dixit et al., 2013). It occurs mainly due to acid attack from food and bacteria buildup (Featherstone, 2008). 'Silver Filling' i.e., dental amalgam containing Hg, Ag, Sn, and Zn (Bharti et al., 2010) has been used as one of the remedies for tooth decay for more than 150 years for filling the cavities (Rathore et al., 2012). But because of harmful and poor aesthetic properties, amalgam became an unfavorable choice as a dental filling material. It affects the brain and kidney functioning because of the release of mercury vapors (Molin, 1992). In modern dentistry, amalgam materials are being replaced by composite materials such as light curing dental composite materials and are being widely spread due to their numerous advantages (Wu et al., 2014). They comprise mainly polymerizable resins, filler particles that are coated with silane coupling agents and photo-initiators (Karabela and Sideridou, 2011). Continuous research and development are going on in this field to improve the chemical, physical, particularly the mechanical properties (Ashour Ahmed et al., 2016), aesthetics (Yu et al., 2009) of these composites. This can be done by altering the parameters such as the type of resin (Ferracane, 1995; Gajewski et al., 2012), and type of fillers (Habib et al., 2016; Miao et al., 2012b), etc. Enhancement of mechanical properties mainly depends on filler factors such as size, shape, and concentration of fillers. Alternatively, new filler particles can be developed (Chevigny et al., 2011) in this field. Filler size is one of the several parameters affecting the overall properties of composite resins (Rastelli et al., 2012).

Nanotechnology has been introduced in the dental field through the production of functional structures in the range of 0.1–100 nm by various physical or chemical methods (Rinastiti et al., 2011). From the past few years, the commercial materials more often possess nanofillers that are claimed to provide superior mechanical properties (de Oliveira et al., 2012). There are various kinds of light curing restorative materials that are available in the market comprising with varying fillers such as nanofilled composite (Khurshid et al.,2015) macro-sized fillers (Filtek Supreme Ultra™), bioactive fillers (Beautifil II™), hybrid fillers (Venus pearl™) and nano-sized fillers (Tetric N-Ceram Ivoclar™). These materials have satisfactory mechanical strength and majorly consist of the filler powders of Si (Balos et al., 2013), Al (Arora et al., 2015), Zn (Sevinç and Hanley, 2010), Zr (Guo et al., 2012) etc. with more than 50 wt% content (Torii et al., 1999). However, there is still a need to overcome the problems of composite materials such as erosion, brittleness, moisture sensitivity, etc (McCabe and Walls, 2013). Titania nanopowder was chosen for this research as it supplies high strength (Awang and Wan Mohd, 2018) to the matrix and has a tooth-like color, good antimicrobial

properties (Pişkin et al.,2013), hydrophilic and self-cleaning nature (Banerjee et al., 2015) to dental materials of the composites. Conventional synthesis methods such as sol-gel (Bessekhouad et al., 2003), thermal decomposition (Moravec et al., 2001), sonochemical (Neppolian et al., 2008) and aerosol formation (Huisman et al., 2003) are time-consuming methods, require harmful chemicals (Tarafdar and Raliya, 2013) and possess higher analysis cost. One of the alternatives to this method is the green synthesis of NPs using renewable sources such as plants (Iravani, 2011). Our work focuses on the efficient method of synthesis of Titania NPs with fruit peel extract and microwave synthesizer to lower the environmental-economic impacts and to promote green chemistry in the field of synthesis of nanoparticles.

Citrus aurantifolia, also known as 'Key lime', is a multipurpose fruit and a rich source of phytoconstituents (Gattuso et al., 2007). Phytoconstituents are responsible for the synthesis of nanoparticles (NPs) during reduction reactions (Santhoshkumar et al., 2017). All phytoconstituents synergistically act as reducing agents and capping agents (Madhumitha et al., 2012) that allow the controlled growth, stability and viability of NPs. Citrus peels can be used in the experimental protocols for the synthesis of NPs (Wilson, 1921). The current research work focuses on the synthesis technique of the TiO$_2$ fillers and their possible use in light curing dental composite materials.

2. Materials and methods

2.1. Materials

C. aurantifolia fruits were collected from a source tree in Bordi, district Palghar, Maharashtra. Peels were dried in an electric oven at 45 °C, finely powdered and sieved (Bansal et al., 2014). Isopropanol, toluene, tetrahydrofuran (THF) and liquor NH$_3$ were commercially available from Alfa Aesar, Mumbai, India. Bisphenol A glycidyl methacrylate (BisGMA), triethylene glycol dimethacrylate (TEGDMA), urethane dimethacrylate (UDMA) and glycidyl methacrylate (GMA) were purchased from Sigma, Mumbai, India. Aminopropyl triethoxysilane (APTES) and photoinitiator camphorquinone (CQ) were purchased from SRL, Mumbai, India.

2.2. Green and rapid synthesis of TiO$_2$ NPs

Fruit peel extract of *C. aurantifolia* was prepared in 10 mL of anhydrous isopropanol by taking 4 g dry powder of the peels. It was then heated to 50 °C under constant stirring for the extraction process in a CEM microwave synthesizer (Zhu and Chen, 2014). The pH of the solution was made alkaline by the addition of liquor NH$_3$ until the pH reached 10. The

precursor of Ti i.e. titanium isopropoxide Ti $\{OCH (CH_3)_2\}_4$ was added to the plant extract during stirring. The solution was then treated under a CEM closed vessel microwave synthesizer at 60 °C for 2 min with the power of 40 W. Evenly dispersed solid particles were produced, indicating the production of NPs. NPs were washed with acetone thrice and calcinated at 450 °C to obtain the final product i.e. green synthesized TiO_2 NPs i.e. $gTiO_2$ NPs.

2.3. Surface modification of gTiO$_2$ NPs

For surface modifications, 1 g solid $gTiO_2$ NPs was dispersed in an enclosed vessel with anhydrous xylene under sonication for 1 h. The nanoparticle suspension was kept at 40 °C under continuous stirring and APTES was added dropwise. The procedure was continued for 5 h. The suspension was then centrifuged following which the filtrate was removed and washed with xylene and finally with acetone thrice. The residue was dried in an oven at 60 °C for complete drying. The dried residue obtained was nano-sized ($\sim$40 nm) APTES modified $gTiO_2$. APTES-modified $gTiO_2$ NPs were then dispersed in anhydrous THF under sonication and then, GMA was added dropwise under continuous sonication for 15 min. The suspension was refluxed at 60 °C for 2 h. The suspension was centrifuged; the filtrate was removed and washed with anhydrous acetone. The process was repeated thrice and then, the residue was dried at 60 °C. The schematic for preparation of GMA-modified $gTiO_2$ NPs ($mTiO_2$) is shown in Fig. 1. The same procedure was repeated with the commercially available titanium dioxide extra pure i.e. microparticles, titanium dioxide nanopowder ($\sim$7 nm) i.e. nanoparticles and the mixture of both i.e. microhybrid particles (SRL, Mumbai, India) for comparison.

2.4. Fabrication of light curing nanocomposite resin material

Experimental light curing resin materials were fabricated as shown in Fig. 2 by mixing different composition of resins, different types of fillers, different amounts, etc. as shown in Tables 1–5, thoroughly for about 6 h. In addition, CQ photo-initiator (2 wt% of the monomer) was added and mixed with the resin matrix using sonication to remove the air gaps in the resin if any. The mixture was then hand mixed rigorously to achieve complete mixing and sonicated again by wrapping the container with aluminum foil to prevent the exposure to light. The materials were prepared in the dimensions required for conducting the specific tests namely compressive, flexural and percentage polymerization shrinkage (% PS) tests. The specimens were prepared in teflon molds of circular and/or rectangular shape. The resin mixture was filled into the molds and sonicated to remove the air bubbles if any. The surface was made smooth by keeping mylar strips™ on it with a glass chip and cured with halogen light of 400–500 nm waveband (3 M ESPE Elipar™2500). The rectangular molds were used for mechanical tests and circular mold was used for polymerization shrinkage.

The light curing machine was held at a distance of 2 mm from the surface of a resin material and cured for 100 s. For samples with a depth of more than 2 mm, the material was cured of both sides for 120 s each to attain complete curing. These samples were prepared in cylindrical molds of dimensions (25 × 2 × 2) mm. For %PS tests, different samples in the circular molds of 7 mm height and 11 mm diameter were prepared. The sample dimensions were calculated and all the experimental samples were kept in distilled water for about 7 days (Thakur et al., 2017) before the analysis. Different sets were prepared by changing the parameters that affect the physical properties of the composite materials such as size of the fillers (Foroutan et al., 2011; Shinkai et al., 2018), amount of fillers (Rastelli et al.,2012), resin matrix (Zhang and Matinlinna, 2011) and surface modification of fillers (Wu et al.,2014). Experimental specimens were divided into 4 sets as mentioned below in Table 1.

The experimental samples were used for mechanical studies i.e. highest compressive, flexural stress and %PS.

2.5. Characterization

Physicochemical characterization of green synthesized nanoparticles and nanocomposite materials was performed by various techniques, namely, dynamic light scattering (DLS), X-ray diffraction (XRD), Fourier Transform Infrared Spectroscopy (FTIR) and Electron Microscopic Techniques. For DLS measurements, samples were diluted in EtOH to 0.1 wt% and data were obtained on DLS model Malvern Nano-ZS (mastersizer software) (Manufacturer- Malvern, United Kingdom) automatically at room temperature. XRD data was obtained by using PANalytical X'pert powder diffractometer (Manufacturer-Philips, Almelo, Netherlands) with the 2Theta values ranging from 20 to 80° using a Cu-Kα source of wavelength of 1.54 Å. The crystallite sizes were
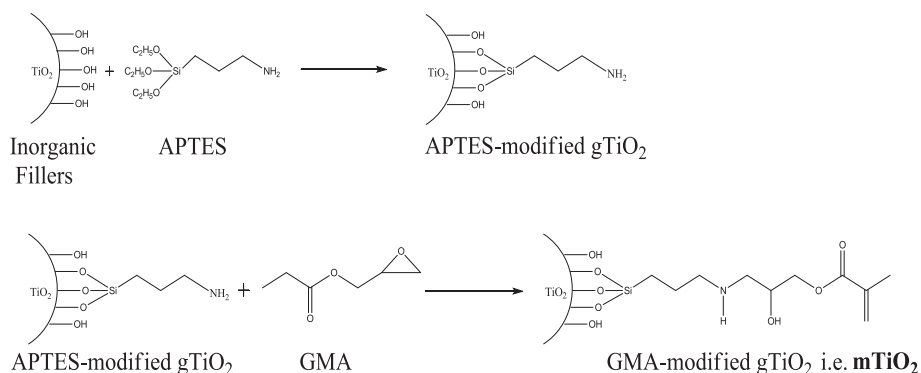

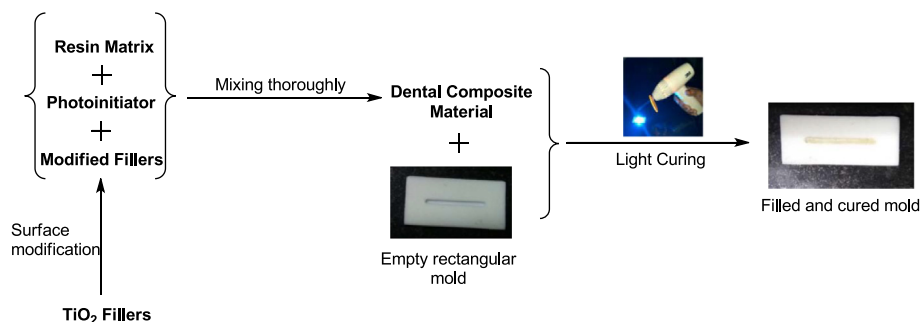**Fig. 1**   Reaction involved in surface modification of gTiO$_2$ nanoparticles.

Fig. 2 Schematic representation of fabrication of light curing dental composite materials.

Table 1 Distribution of four sets with composition of resin, different fillers type, wt% of fillers and nature for the fabrication of experimental samples.

Set	Resin Material	Filler Type	Wt% of Filler	Nature
1	BisGMA 100 wt%	Micro, microhybrid, nano, nanohybrid	10	mTiO$_2$
2	BisGMA 100 wt%	Nanohybrid particles	0, 1, 2, 510	mTiO$_2$
3	Different composition of resins	Nanohybrid particles	5	mTiO$_2$
4	BisGMA 60 wt% + TEGDMA 20 wt% + UDMA 20 wt%	Nanohybrid particles	5	mTiO$_2$ & bare gTiO$_2$

gTiO$_2$ = green synthesized TiO$_2$ NPs; mTiO$_2$ = surface modified gTiO$_2$.

Table 2 Set 1: Physical properties of dental materials with different types of fillers.

Resin materials	Type of mTiO$_2$ fillers	Wt% of fillers mTiO$_2$	Max. compressive stress (MPa)[*]	Max. flexural stress (MPa)[*]	% PS[*]
BisGMA 100 wt%	Micro	10	76.97 ± 0.27	32.12 ± 0.02	10.50 ± 0.18
	Microhybrid		90.50 ± 0.43	31.50 ± 0.43	12.95 ± 0.52
	Nano		91.25 ± 0.22	50.98 ± 0.23	6.82 ± 0.07
	Nanohybrid		141.95 ± 0.91	52.92 ± 0.69	7.48 ± 0.14

mTiO$_2$: surface modified gTiO$_2$.

[*] Mean of three readings ± S.D.

calculated from the Scherrer formula applied to the major intense peaks (Mahshid et al., 2007). FTIR spectra were recorded on IR Prestige 2, (Manufacturer-Shimadzu, Kyoto, Japan) in the range of 400–4000 cm^{-1} to determine the chemical bonding in the organic components present over the surface of nanoparticles after surface modification. Morphology and surface images were taken on Transmission Electron Microscope (TEM)-CM200 equipped with Selected Area Electron Diffraction (SAED) (Manufacturer- Philips, Madison, United States), Scanning Electron Microscope (SEM) with Energy Dispersive X-ray Spectroscopy (EDS) (Manufacturer-Zeiss, Stockholm, Sweden) with a focused electron beam to deliver images with information about the sample's topography, size by SEM and elemental composition by EDS.

Experimental light curing specimens were tested for their mechanical properties. The hardness of the particles has a great influence on compressibility. Higher flexural stress that a material can bear was obtained through a three-point bending test in order to figure out the ability of the sample to withstand the bending forces applied (Sfondrini et al., 2014).

Polymerization shrinkage (PS) of resin-composite materials may have a negative impact on the clinical performance (Braga et al., 2005) and thus a reduction in % PS is required (Karaman and Ozgunaltay, 2014). The objective of this study was to obtain an efficient protocol for the green synthesized TiO$_2$ NPs for the enhancement of physical properties of the light curing resin materials. Compression and flexural tests (Sfondriniet al.,2014) were performed using Universal Testing Machine, Instron 3345 with a capacity of 5000 N having the test speed of 0.5 mm/min on Bluehill 3 software. Compression tests were performed for cylindrical specimens having dimensions of 5 mm diameter and 5 mm height prepared by a teflon mold. The specimen was placed on its end between the plates of the universal testing machine. The compressive load was applied along the long axis of the specimen at a cross-head speed of 0.5 mm/min until the material breaks.

The flexural test was performed with the help of universal testing machine for obtaining maximum flexure load, flexure stress at maximum load, and maximum flexure strain values. The sample was mounted in the testing device using rounded

Table 3 Set 2: Physical properties of dental materials with increase in wt% of fillers.

Resin materials	Type of mTiO$_2$ fillers	Wt% of mTiO$_2$ fillers	Max. compressive stress (MPa)[*]	Max. flexural stress (MPa)[*]	% PS[*]
BisGMA 100 wt%	Nanohybrid	0	24.58 ± 0.47	3.82 ± 0.07	16.5 ± 0.21
		1	54.09 ± 0.23	13.97 ± 0.13	12.5 ± 0.47
		2	91.1 ± 1.47	18.90 ± 0.30	9.11 ± 0.08
		5	158.28 ± 1.43	61.78 ± 1.20	8.17 ± 0.47
		10	141.95 ± 0.91	52.92 ± 0.69	7.48 ± 0.14

mTiO$_2$: surface modified gTiO$_2$.
[*] Mean of three readings ± S.D.

Table 4 Set 3: Physical properties of dental materials with different resins composition.

Resin materials	Type of mTiO$_2$ fillers	Wt% of mTiO$_2$ fillers	Max. compressive stress (MPa)[*]	Max. flexural stress (MPa)[*]	% PS[*]
BisGMA 100 wt%	Nanohybrid	5	158.28 ± 1.43	61.78 ± 1.20	8.17 ± 0.47
BisGMA 60 wt% + TEGDMA 40 wt%			155.28 ± 1.07	66.03 ± 0.28	5.21 ± 0.32
BisGMA 60 wt% + UDMA 40 wt%			199.78 ± 0.92	79.98 ± 0.18	6.15 ± 0.15
BisGMA 60 wt% + TEGDMA 20 wt% + UDMA 20 wt%			195.55 ± 0.75	83.30 ± 0.07	3.48 ± 0.29

mTiO$_2$: surface modified gTiO$_2$.
[*] Mean of three readings ± S.D.

Table 5 Set 4: Physical properties of dental materials with bare Vs surface modified fillers.

Resin materials	Type of fillers	Max. compressive stress (MPa)[*]	Max. flexural stress (MPa)[*]	% PS[*]
BisGMA 60 wt% + TEGDMA 20 wt% + UDMA 20 wt%	5 wt% Nanohybrid Bare TiO$_2$	100.32 ± 0.20	70.65 ± 0.55	4.12 ± 0.04
BisGMA 60 wt% + TEGDMA 20 wt% + UDMA 20 wt%	5 wt% Nanohybrid mTiO$_2$	195.55 ± 0.75	83.30 ± 0.07	3.48 ± 0.29

mTiO$_2$: surface modified gTiO$_2$.
[*] Mean of three readings ± S.D.

supports at a distance of 20 mm and the beams were loaded until failure using the across-head speed of 0.5 mm/min (Hahnel et al., 2010) and operated until the material breaks.

For polymerization shrinkage, % PS values were obtained after weighing the samples and calculated by the following formula:

$$[(V_1 - V_2)/V_2] \times 100 = \% \text{ PS} \ \& \ V_1 = M_1/D_1; V_2 = M_2/D_2$$

where,

V = Volume of resin before (V$_1$) & after (V$_2$) curing
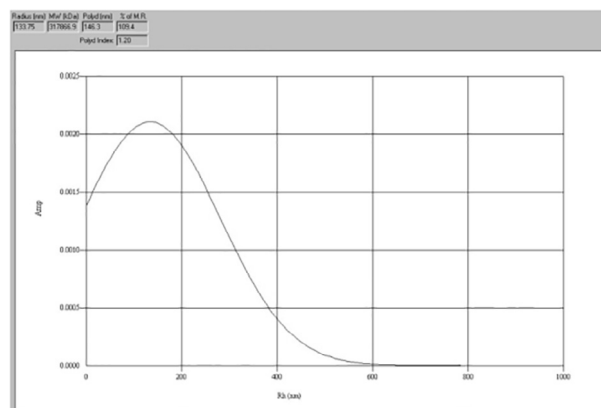M = Mass of resin before (M$_1$) & after (M$_2$) curing
D = Density of resin before (D$_1$) & after (D$_2$) curing

3. Results

3.1. DLS

Graph of Amp Vs Rh (hydrodynamic radius) in nanometer range gave the average radius of suspended particles as 133.75 nm that indicates the presence of micro-sized gTiO$_2$ particles. The polydispersity index of the data obtained is 146.3 nm (Fig. 3).
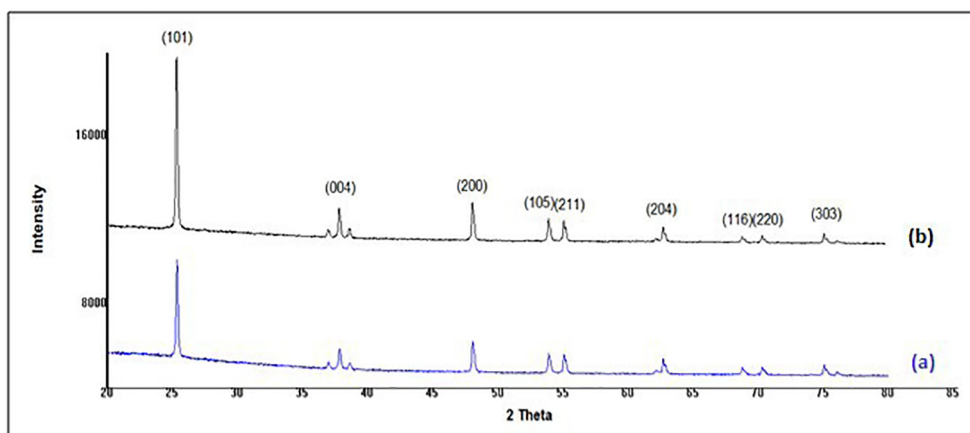

Fig. 3 DLS spectrum of gTiO$_2$ NPs.

Fig. 4 XRD pattern of (a) bare gTiO₂ NPs (b) APTES-coated gTiO₂ NPs.

3.2. Crystallite size and phase identification by XRD

Identification of phases of samples bare gTiO₂ (a) and APTES-coated gTiO₂ (b) was determined by matching peak positions and intensities of the peak with reference (JCPDS card no. 88-1175), as shown in the Fig. 4. The absence of spurious diffraction indicates the crystallographic purity of bare and coated gTiO₂ NPs, and sharp peaks indicate the crystalline nature of particles. Major 2θ peaks of 25.3°, 38.0°, 48.1°, and 54.7° were seen in Fig. 4 lines (a) and (b) that resemble the characteristic anatase TiO₂ structure. The comparison of two XRD patterns pre (line a) and post APTES coating (line b) illustrate that the silane group has no impact on the crystal structure of TiO₂ and the coating was properly done on the particles, thus showing no extra peaks and high anatase phase purity. The size of the crystalline domain based on the most intense peaks of line (a) and (b) were found to be 30.09 nm and 40.73 nm, respectively.

3.3. FTIR

The FTIR spectrum of bare gTiO₂ NPs Fig. 5 (line a) and APTES-coated gTiO₂ NPs (line b) was compared to confirm APTES coating on the sur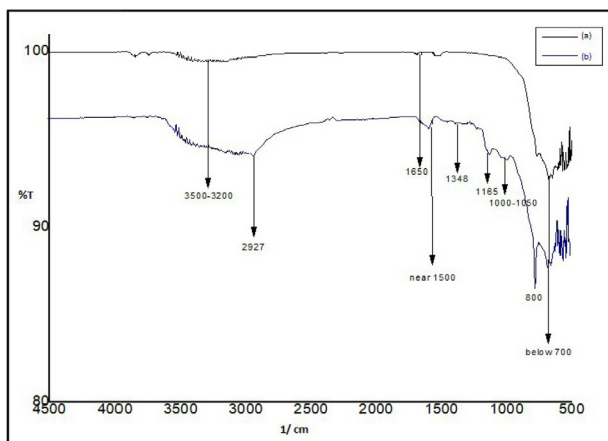face of gTiO₂. The FTIR spectrum of bare gTiO₂ NPs (a) showed a wide broadband at 3200–3500 cm^{-1} due to the stretching vibration of water molecules adsorbed on the surface of hydrophilic gTiO₂NPs. The small peak at 1650 cm^{-1} was attributed to ─OH bending vibrations. Many peaks below 700 cm^{-1} were present because of the numerous of Ti─O─Ti bonds in bare gTiO₂ NPs. APTES coated gTiO₂ NPs (b) showed a broad band at 3500–3200 cm^{-1} due to the presence of ─OH molecules on to the surface of gTiO₂ NPs and N─H symmetrical stretching. A weak band at 2927 cm^{-1} indicates the presence of alkyl groups [─(CH₂)$_n$─]. The absorption band near 1500 cm^{-1} corresponded to ─N─H vibrations in amino group of APTES. A peak at 1024 cm^{-1} was because of the stretching vibrations of Ti─O─Si moieties and the peak at 1348 cm^{-1} was ascribed to C─N stretching mode present in the range of 1000–1050 cm^{-1} while the broadband at1165 cm^{-1}is ascribed to Si─O─Si stretching. The peak at 800 cm^{-1} corresponded to Si─C stretching and NH₂ out-of-plane bending mode, confirming the APTES coating on the bare gTiO₂ NPs, as shown in Fig. 5.

3.4. SEM and EDS

SEM image represented the spherical nature of gTiO₂ NPs of different sizes. Image consisted small i.e. nano and micro-sized particles, as shown in Fig. 6(a). The particles were aggregated due to the effect of Vander Waals forces existing in small sized particles. The particle size from SEM was obtained in the range of 3 nm to 1 μm, marked in Fig. 6(a), indicated the nanohybrid nature of particles.

Impurities that can be present in the TiO₂ samples have been evaluated with the EDS techniques. The EDS data (the contents of Ti, O and the impurity atoms on the sample surface) were obtained at different points at the TiO₂ surface. It was noticed that the EDS data of pure TiO₂ Fig. 6(b). The abscissa of the EDS spectrum indicates the ionization energy and ordinate indicates the counts. Higher the counts of a particular element, higher will be its presence at that point or area of interest or vice a versa.

3.5. TEM

The particle size estimated from TEM Fig. 7(a), (b) and (c), were found to be in the range of 10–100 nm as shown in
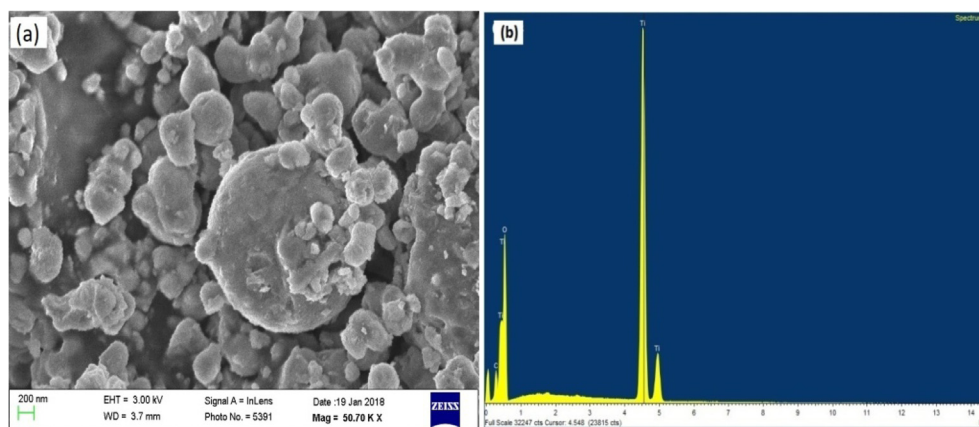

Fig. 5 FTIR image of (a) bare gTiO₂ NPs (b) APTES coated gTiO₂ NPs.

Fig. 6 (a) SEM image of green synthesized gTiO₂ nanohybrid particles (b) EDS spectra for gTiO₂ nanohybrid particles.
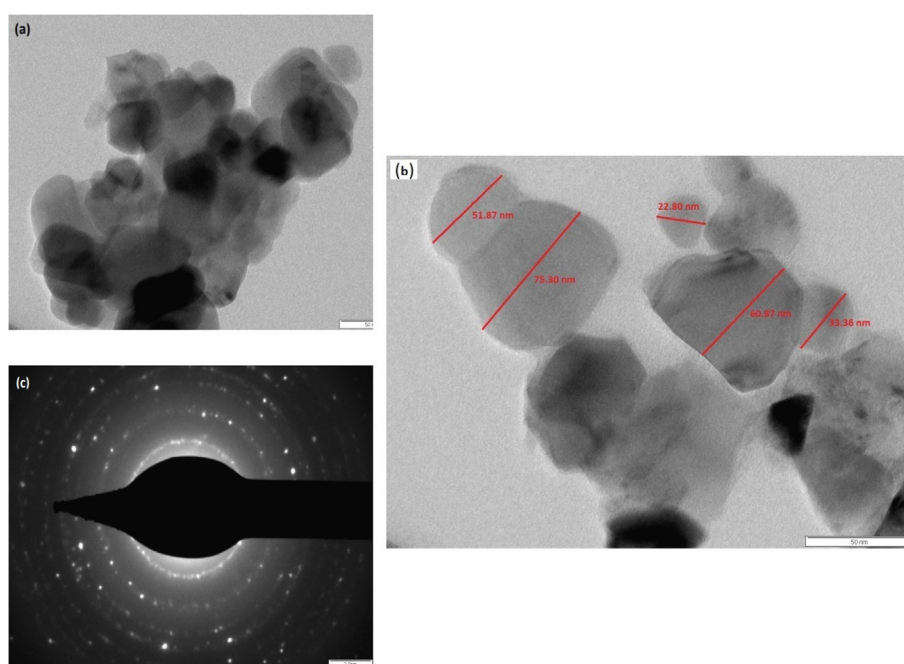

Fig. 7 TEM images of (a) bare gTiO₂ NPs (b) APTES coated gTiO₂ NPs (c) SAED pattern of APTES coated gTiO₂ NPs.

Fig. 7(a), bare gTiO₂ NPs were highly aggregated and no distinct particles were found where as in Fig. 7(b), APTES coated gTiO₂ NPs were well separated from each other and reduced aggregation was observed between nano and micro-sized particles indicating nanohybrid nature of APTES-coated gTiO₂ NPs. Fig. 7(c) represented the SAED pattern of APTES-coated gTiO₂ NPs and showed that the small spots form rings, indicated polynanocrystalline nature.

3.6. Physical properties of dental materials

The results of the physical properties of dental materials of the materials, namely, maximum compressive stress, flexural stress and % PS of all four sets of samples listed in Table 1 are shown in Tables 2–5. The samples were analyzed thrice. Mean of the three readings (n = 3) with standard deviation (S.D.) are mentioned in the following tables.

Effect of different types of fillers is represented in the Table 2 (set 1) with the resin material (BisGMA 100 wt%) and amount of fillers (10 wt%) constant.

The type of filler that gave higher mechanical strength (maximum compressive and flexural stress) i.e. nanohybrid surface modified fillers, were used for next sets.

Effect of different wt% of nanohybrid fillers is represented in Table 3 (set 2) with the resin material (BisGMA 100 wt%) and type of fillers (nanohybrid) constant.

The amount of nanohybrid fillers that gave higher mechanical strength (Maximum compressive and flexural stress) was used for next sets i.e. 5 wt% mTiO₂ nanohybrid fillers.

Effect of different composition of resin materials viz. BisGMA, UDMA, TEGDMA with varying percentage composition, etc. was carried out in Table 4 (set 3) with the type of mTiO₂ fillers (nanohybrid) and amount of fillers (5 wt%) were kept constant.

Table 6 Final result of experimental composite material with the highest mechanical strength (direct measurement) and lowest % polymerization shrinkage.

Resin material	Fillers	Max. compressive stress (MPa)[*]	Max. flexural stress (MPa)[*]	% PS[*]
BisGMA 60 wt% + TEGDMA 20 wt% + UDMA 20 wt%	Nanohybrid 5 wt% mTiO$_2$	195.56	83.30	3.48

mTiO$_2$: surface modified gTiO$_2$.
[*] Mean of three readings.

The composition of resin matrix which gave higher mechanical strength (maximum compressive and flexural stress) and lower % polymerization shrinkage was used for further testing i.e. BisGMA 60 wt% + TEGDMA 20 wt% + UDMA 20 wt%.

Effect of surface modification on mechanical and dental properties of experimental composite materials with 5 wt% nanohybrid mTiO$_2$; resin composition BisGMA 60 wt% + TEGDMA 20 wt% + UDMA 20 wt% was carried out as represented in Table 4.5 (set 4).

The experimental nanocomposites material with 5 wt% surface modified nanohybrid fillers (mTiO$_2$) gave higher mechanical strength (maximum compressive, flexural stress) and lower % polymerization shrinkage and as compared to the material without surface modified nanofillers mTiO$_2$.

Set 1 Table 2 represented dental composite material with nanohybrid fillers possessing higher compressive stress 141.95 MPa and flexural stress 52.92 MPa and lower % PS i.e. 7.48% than micro, microhybrid and nanosized fillers.

Set 2 Table 3 represented 5 wt% mTiO$_2$ nanohybrid fillers gave higher mechanical strength i.e. 158.28 MPa compressive stress, 61.78 MPa flexural stress as compared to 0 wt%, 1 wt%, 2 wt%, 10 wt% mTiO$_2$ nanohybrid fillers.

In set 3 Table 4, the mixture of three resins BisGMA 60 wt% + UDMA 20 wt% + TEGDMA 20 wt% with 5 wt% nanohybrid fillers possessed compressive stress 195.55 MPa which is lower than that of resin composition BisGMA 60 wt% + UDMA 40 wt%. But, % PS shrinkage was least i.e. 3.48% in mixture of three resins which was desired.

Set 4 Table 5 represented the comparative result of material with bare and surface modified 5 wt% nanohybrid fillers in which surface modified fillers gave compressive stress 195.55 MPa, flexural stress 83.30 MPa, and lowest % PS 3.48% as compared to the nanocomposite material surface modified fillers. The optimized result of the material which gave the highest mechanical strength and lowest desired % PS by considering all 4 sets is shown in Table 6.

4. Discussion

Physiochemical characterization showed that the green microwave synthesized particles gTiO$_2$ were a mixture of nano and micro-sized particles i.e. nanohybrid in nature. Temperature and pressure parameters were controlled in the compact microwave synthesizer, and this rapid process allowed the size-controlled synthesis to take place in a few minutes.

Microwave process has high efficiency (Zhu and Chen, 2014), consumes less energy and reduces time, with enhancement in quality of the product. The size of gTiO$_2$ particles was 146.3 nm i.e. in micrometer, which was concluded from

DLS system. In general, TiO$_2$ particles possess excellent biocompatibility and decrease the potential of an allergic reaction (Hilger, 2013). APTES-coated gTiO$_2$ were responsible for the reduction in the aggregation of particles even when dispersion into the resin matrix. In the GMA-modified gTiO$_2$, the C≡C group of GMA on the surface of gTiO$_2$ could participate in the polymerization of the monomer and form a covalent linkage in the resin matrix and fillers, thus helping in the improvement of mechanical strength of the material (Rastelli et al., 2012; Shinkai et al.,2018). In case of % PS, the volume contraction is dependent on many factors including filler concentration (de Melo Monteiro et al., 2011). Low polymerization shrinkage (% PS) value indicated less micro-leakage and better restoration (Li et al., 2012). The results of other physical properties of dental materials of the experimental composite materials showed that the nanohybrid fillers were excellent among micro, micro hybrid and nano-sized fillers (Table 2). This may be because these fillers depicted the properties of both and they are hard to dislodge the small particles from the gaps of micro-sized particles. The mechanical properties of the final resin material was improved with an increase in wt% of fillers and showed the highest value at 5 wt% (Table 3). This may be because the increase in the number of fillers increases agglomeration, which in turn affects the mechanical strength of the resin (Rastelli et al., 2012). The mixture of the three resins together gave higher values of strength than that of the single resin or mixture of two (Table 4) and thus the surface-modified NPs were apt as dental nanocomposites rather than bare fillers (Table 5).

On comparing the mechanical data of green synthesized fillers with the similar work carried out by Wu and coworkers, it was observed that gTiO$_2$ fillers achieved reduction of % PS value to 3.48% which is lesser than that of 5.9% (Wu et al., 2014). This may be due to the stepwise selection of nanohybrid fillers, optimum wt% of surface modified fillers and optimum resin composition. Also, the final material (Table 6) showed considerable increase in mechanical strength than of the conventional amalgam material (Narasimha and Vinod, 2013).

Dental nanocomposites have provided cosmetically acceptable results with excellent mechanical properties for both bulk (Rinastiti et al., 2010) and fiber reinforced materials (Scribante et al., 2015). Researchers are synthesizing SiO$_2$ microspheres (Miao et al., 2012a), zirconia-silica nanofibres (Guo et al., 2012), alumina (Arora et al., 2015), etc. as fillers and some have also worked upon their synthesis for the purpose of dental composites e.g. nanosilica by chemical method (Canché-Escamilla et al., 2014) and ZrO$_2$/Al$_2$O$_3$ fillers by CO$_2$ laser co-vaporization (Bartolomé et al., 2016), which are purely chemical methods. We have used 'Green Nanotechnology' concept in the field of synthesis of dental fillers.

Considering the facts of TiO$_2$ exposure in human body, 5 wt% of TiO$_2$ has minimal effects on health compared with the other composites with higher filler content (e.g., 65 wt% of silica in Vertise Flow™ (Maas et al., 2017), 78 wt% filler content in Filtek supreme™ (França et al., 2014). Future studies in this field could involve other important aspects of nanofiller characteristics, such as cytotoxicity, color shades, color stability, *in vitro* studies. Moreover, evaluation of cytotoxicity of the as-prepared resin composite material and NPs in oral proximity and its clinical performance is needed in future.

5. Conclusion

The results indicated that green synthesized and surface modified 5 wt% (mTiO$_2$) nanohybrid particles in the resin mixture of bisphenol A glycidyl methacrylate (60 wt%), triethylene glycol dimethacrylate (20 wt%), urethane dimethacrylate (20 wt%) gives increased mechanical strength and decreased percentage polymerization shrinkage among the different sets of experimental compositions. In addition to the antimicrobial, hydrophilic and self-cleaning nature of tooth colored TiO$_2$ nanoparticles; gTiO$_2$ nanohybrids can be used as effective fillers for light curing dental nanohybrid composite materials for improving their physical properties.

Conflict of interest

The authors declared that there is no conflict of interest

Acknowledgement

References

Arora, P., Singh, S.P., Arora, V., 2015. Effect of alumina addition on properties of polymethylmethacrylate–a comprehensive review. Int. J. Biotech. Trends Technol. 9, 1–7.

Ashour Ahmed, M., El-Shennawy, M., Althomali, Y., Omar, A.A., 2016. Effect of titanium dioxide nano particles incorporation on mechanical and physical properties on two different types of acrylic resin denture base. World J. Nano Sci. Eng. 06, 111–119.

Awang, M., Wan Mohd, W.R., 2018. Comparative studies of titanium dioxide and zinc oxide as a potential filler in polypropylene reinforced rice husk composite. IOP Conf. Ser. Mater. Sci. Eng. 342, 012046.

Balos, S., Pilic, B., Petronijevic, B., Markovic, D., Mirkovic, S., Sarcev, I., 2013. Improving mechanical properties of flowable dental composite resin by adding silica nanoparticles. Vojnosanit. Pregl. 70, 477–483.

Banerjee, S., Dionysiou, D.D., Pillai, S.C., 2015. Self-cleaning applications of TiO$_2$ by photo-induced hydrophilicity and photocatalysis. Appl. Catal. B Environ. 176–177, 396–428.

Bansal, J., Malviya, R., Malaviya, T., Bhardwaj, V., Sharma, P.K., 2014. Evaluation of banana peel pectin as excipient in solid oral. Dosage Form 4.

Bartolomé, J.F., Smirnov, A., Kurland, H.-D., Grabow, J., Müller, F.A., 2016. New ZrO$_2$/Al$_2$O$_3$ nanocomposite fabricated from hybrid nanoparticles prepared by CO$_2$ laser co-vaporization. Sci. Rep. 6, 20589.

Bessekhouad, Y., Robert, D., Weber, J.V., 2003. Preparation of TiO$_2$ nanoparticles by sol-gel route. Int. J. Photoenergy 5, 153–158.

Bharti, R., Wadhwani, K.K., Tikku, A.P., Chandra, A., 2010. Dental amalgam: an update. J. Conserv. Dent. JCD 13, 204–208.

Braga, R., Ballester, R., Ferracane, J., 2005. Factors involved in the development of polymerization shrinkage stress in resin-composites: a systematic review. Dent. Mater. 21, 962–970.

Canché-Escamilla, G., Duarte-Aranda, S., Toledano, M., 2014. Synthesis and characterization of hybrid silica/PMMA nanoparticles and their use as filler in dental composites. Mater. Sci. Eng. C 42, 161–167.

Chevigny, C., Jouault, N., Dalmas, F., Boué, F., Jestin, J., 2011. Tuning the mechanical properties in model nanocomposites: influence of the polymer-filler interfacial interactions. J. Polym. Sci. Part B Polym. Phys. 49, 781–791.

de Melo Monteiro, G.Q., Montes, M.A.J.R., Rolim, T.V., de Oliveira Mota, C.C.B., de Barros Correia Kyotoku, B., Gomes, A.S.L., de Freitas, A.Z., 2011. Alternative methods for determining shrinkage in restorative resin composites. Dent. Mater. Off. Publ. Acad. Dent. Mater. 27, E176–E185.

De Oliveira, G.U., Mondelli, R.F.L., Charantola Rodrigues, M., Franco, E.B., Ishikiriama, S.K., Wang, L., 2012. Impact of filler size and distribution on roughness and wear of composite resin after simulated toothbrushing. J. Appl. Oral Sci. 20, 510–516.

Featherstone, J., 2008. Dental caries: a dynamic disease process. Aust. Dent. J. 53, 286–291.

Ferracane, J.L., 1995. Current trends in dental composites. Crit. Rev. Oral Biol. Med. 6, 302–318.

Foroutan, F., Javadpou, J., Atai, M., Rezaie, H.R., et al, 2011. Mechanical properties of dental composite materials reinforced with micro and nano-size Al$_2$O$_3$ filler particles. Iran. J. Mater. Sci. Eng. 8, 25–33.

França, F.M., Rodrigues, J., Turssi, C., Bandeira de Andrade, I.C., Basting, R., do Amaral, F.L., 2014. Microhardness and color monitoring of nanofilled resin composite after bleaching and staining. Eur. J. Dent. 8, 160.

Gajewski, V.E., Pfeifer, C.S., Fróes-Salgado, N.R., Boaro, L.C., Braga, R.R., 2012. Monomers used in resin composites: degree of conversion, mechanical properties and water sorption/solubility. Braz. Dent. J. 23, 508–514.

Gattuso, G., Barreca, D., Gargiulli, C., Leuzzi, U., Caristi, C., 2007. Flavonoid composition of citrus juices. Molecules 12, 1641–1673.

Guo, G., Fan, Y., Zhang, J.-F., Hagan, J.L., Xu, X., 2012. Novel dental composites reinforced with zirconia-silica ceramic nanofibers. Dent. Mater. Off. Publ. Acad. Dent. Mater. 28, 360–368.

Habib, E., Wang, R., Wang, Y., Zhu, M., Zhu, X.X., 2016. Inorganic fillers for dental resin composites: present and future. ACS Biomater. Sci. Eng. 2, 1–11.

Hahnel, S., Henrich, A., Bürgers, R., Handel, G., Rosentritt, M., 2010. Investigation of mechanical properties of modern dental composites after artificial aging for one year. Oper. Dent. 35, 412–419.

Hilger, I., 2013. Biocompatibility of Titanium Dioxide Nanoparticles for Diagnostic and Therapeutic Purposes in Personalized Nanomedicine.

Huisman, C.L., Goossens, A., Schoonman, J., 2003. Aerosol synthesis of anatase titanium dioxide nanoparticles for hybrid solar cells. Chem. Mater. 15, 4617–4624.

Iravani, S., 2011. Green synthesis of metal nanoparticles using plants. Green Chem. 13, 2638–2650.

Karabela, M.M., Sideridou, I.D., 2011. Synthesis and study of properties of dental resin composites with different nanosilica particles size. Dent. Mater. 27, 825–835.

Karaman, E., Ozgunaltay, G., 2014. Polymerization shrinkage of different types of composite resins and microleakage with and without liner in class II cavities. Oper. Dent. 39, 325–331.

Khurshid, Z., Zafar, M., Qasim, S., Shahab, S., Naseem, M., AbuRequaiba, A., Rehman, 2015. Advances in nanotechnology for restorative dentistry. Materials 8 (2), 717–731.

Li, Y., Sun, X., Chen, J., Xiong, J., Hu, X., 2012. Polymerization shrinkage/stress and dentin bond strength of silorane and dimethacrylate-based dental composites. J. Appl. Polym. Sci. 124, 436–443.

Maas, M.S., Alania, Y., Natale, L.C., Rodrigues, M.C., Watts, D.C., Braga, R.R., Maas, M.S., Alania, Y., Natale, L.C., Rodrigues, M.C., Watts, D.C., Braga, R.R., 2017. Trends in restorative composites research: what is in the future? Braz. Oral Res., 31

Madhumitha, G., Rajakumar, G., Roopan, S.M., Rahuman, A.A., Priya, K.M., Saral, A.M., Khan, F.R.N., Khanna, V.G., Velayutham, K., Jayaseelan, C., Kamaraj, C., Elango, G., 2012. Acaricidal, insecticidal, and larvicidal efficacy of fruit peel aqueous extract of Annona squamosa and its compounds against blood-feeding parasites. Parasitol. Res. 111, 2189–2199.

Mahshid, S., Askari, M., Ghamsari, M.S., 2007. Synthesis of TiO$_2$ nanoparticles by hydrolysis and peptization of titanium isopropoxide solution. J. Mater. Process. Technol. 189, 296–300.

McCabe, J.F., Walls, A.W.G., 2013. Applied Dental Materials. John Wiley & Sons.

Miao, X., Li, Y., Zhang, Q., Zhu, M., Wang, H., 2012a. Low shrinkage light curable dental nanocomposites using SiO$_2$ microspheres as fillers. Mater. Sci. Eng. C 32, 2115–2121.

Miao, X., Zhu, M., Li, Y., Zhang, Q., Wang, H., 2012b. Synthesis of dental resins using diatomite and nano-sized SiO$_2$ and TiO$_2$. Prog. Nat. Sci. Mater. Int. 22, 94–99.

Molin, C., 1992. Amalgam – fact and fiction. Eur. J. Oral Sci. 100, 66–73.

Moravec, P., Smolík, J.V., Levdansky, V., 2001. Preparation of TiO$_2$ fine particles by thermal decomposition of titanium tetraisopropoxide vapor. J. Mater. Sci. Lett. 20, 2033–2037.

Narasimha, J., Vinod, V., 2013. Comparative evaluation of compressive strength and flexural strength of conventional core materials with nanohybrid composite resin core materials with nanohybrid composite resin core material an invitro study. J. Ind. Prosthodont. Soc. 13 (3), 281–289.

Neppolian, B., Wang, Q., Jung, H., Choi, H., 2008. Ultrasonic-assisted sol-gel method of preparation of TiO$_2$ nano-particles: characterization, properties and 4-chlorophenol removal application. Ultrason. Sonochem. 15, 649–658.

Pişkin, S., Palantöken, A., Yılmaz, M.S., 2013. Antimicrobial Activity of Synthesized TiO2 Nanoparticles 4.

Prasai Dixit, L., Shakya, A., Shrestha, M., Shrestha, A., 2013. Dental caries prevalence, oral health knowledge and practice among indigenous Chepang school children of Nepal. BMC Oral Health 13, 20.

Rastelli, A.N.S., Jacomassi, D.P., Faloni, A.P.S., Queiroz, T.P., Rojas, S.S., Bernardi, M., Inê, B., Bagnato, V.S., Hernandes, A.C., 2012. The filler content of the dental composite resins and their influence on different properties. Microsc. Res. Tech. 75, 758–765.

Rathore, M., Singh, A., Pant, V.A., 2012. The dental amalgam toxicity fear: a myth or actuality. Toxicol. Int. 19, 81.

Rinastiti, M., Ozcan, M., Siswomihardjo, W., Busscher, H.J., 2010. Immediate repair bond strengths of microhybrid, nanohybrid and nanofilled composites after different surface treatments. J. Dent. 38, 29–38.

Rinastiti, M., Özcan, M., Siswomihardjo, W., Busscher, H.J., 2011. Effects of surface conditioning on repair bond strengths of non-aged and aged microhybrid, nanohybrid, and nanofilled composite resins. Clin. Oral Investig. 15, 625–633.

Santhoshkumar, J., Rajeshkumar, S., Venkat Kumar, S., 2017. Phyto-assisted synthesis, characterization and applications of gold nanoparticles – a review. Biochem. Biophys. Rep. 11, 46–57.

Scribante, A., Massironi, S., Pieraccini, G., Vallittu, P., Lassila, L., Sfondrini, M.F., Gandini, P., 2015. Effects of nanofillers on mechanical properties of fiber-reinforced composites polymerized with light curing and additional postcuring. J. Appl. Biomater. Funct. Mater. 13, e296–e299.

Sevinç, B.A., Hanley, L., 2010. Antibacterial activity of dental composites containing zinc oxide nanoparticles. J. Biomed. Mater. Res. B Appl. Biomater. 94, 22–31.

Sfondrini, M.F., Massironi, S., Pieraccini, G., Scribante, A., Vallittu, P.K., Lassila, L.V., Gandini, P., 2014. Flexural strengths of conventional and nanofilled fiber-reinforced composites: a three-point bending test. Dent. Traumatol. Off. Publ. Int. Assoc. Dent. Traumatol. 30, 32–35.

Shinkai, K., Taira, Y., Suzuki, S., Kawashima, S., Suzuki, M., 2018. Effect of filler size and filler loading on wear of experimental flowable resin composites. J. Appl. Oral Sci., 26

Tarafdar, J.C., Raliya, R., 2013. Rapid, low-cost, and ecofriendly approach for iron nanoparticle synthesis using *Aspergillus oryzae* TFR9. J. Nanoparticles 2013, 1–4.

Thakur, V.K., Thakur, M.K., Kessler, M.R., 2017. Handbook of Composites from Renewable Materials, Nanocomposites: Science and Fundamentals. John Wiley & Sons.

Torii, Y., Itou, K., Itota, T., Hama, K., Konishi, N., Nagamine, M., Inoue, K., 1999. Influence of filler content and gap dimension on wear resistance of resin composite luting cements around a CAD/CAM ceramic inlay restoration. Dent. Mater. J. 18, 453–461.

Wilson, C.P., 1921. The manufacture of citric acid from lemons. J. Ind. Eng. Chem. 13, 554–558.

Wu, M., Zhang, F., Yu, J., Zhou, H., Zhang, D., Hu, C., Huang, J., 2014. Fabrication and evaluation of light curing nanocomposite resins filled with surface-modified TiO$_2$ nanoparticles for dental application. Iran. Polym. J. 23, 513–524.

Yu, B., Ahn, J.-S., Lim, J.I., Lee, Y.-K., 2009. Influence of TiO$_2$ nanoparticles on the optical properties of resin composites. Dent. Mater. 25, 1142–1147.

Zhang, M., Matinlinna, J.P., 2011. The effect of resin matrix composition on mechanical properties of e-glass fiber-reinforced composite for dental use. J. Adhes. Sci. Technol. 25, 2687–2701.

Zhu, Y.-J., Chen, F., 2014. Microwave-assisted preparation of inorganic nanostructures in liquid phase. Chem. Rev. 114, 6462–6555.